SLIP ALONG THE SUPERSTITION HILLS FAULT ASSOCIATED WITH THE 24 NOVEMBER 1987 SUPERSTITION HILLS, CALIFORNIA, EARTHQUAKE

By Patrick L. Williams and Harold W. Magistrale

ABSTRACT

Surficial slip along the entire mapped length of the Superstition Hills fault in southern California occurred in association with the Superstition Hills earthquake (M_s 6.6) of 24 November 1987. We made repeated measurements of surface slip at 36 sites along the fault and occupied 64 sites at least once. At our sites, dextral slip was as high as 48.5 cm 1 day after the earthquake and 71 cm 2 months after. The measurements show that slip during the period from hr to several hundred hr following the event is described by a simple power law of time. Extrapolation to $t = 1$ min indicates that co-seismic slippage ranged from 5 to 23 cm at 10 of our best recorded sites, suggesting that finite co-seismic slippage occurred along the length of the fault. These extrapolations are supported by a measurement made at Imler Road 30 min after the shock.

Measurements are complete through October 1988. At many sites, the form of slip-rate was decay changed from power law to a function of log time during the interval between 300 and 500 hr after the earthquake. Logarithmic slip-rate decay in time was observed for a period of several yr after the Parkfield, Borrego Mountain, and Imperial Valley earthquakes. Those measurements may have begun too late to resolve power-law behavior at early times. If current logarithmic behavior of the Superstition Hills fault persists, right-lateral slippage will approach 90 cm 10 yr after the rupture.

Changes in the along-fault displacement profile correlate well with geometric features including a fault bend and a major fault step. Moreover, slip behavior appears to be correlated to the thickness of sedimentary cover along the fault. Also, the northern half of the fault is bounded by a large block of continental crystalline basement. The presence of this block may have contributed to the relatively uniform early slip behavior observed there.

INTRODUCTION

The 24 November M_s 6.6 Superstition Hills earthquake was part of a complex sequence of earthquakes in late 1987. Kahle et al. (1988) found no slippage across the Superstition Hills fault during a visit about 2.5 hr before the Superstition Hills earthquake, but they observed dextral surface displacement of about 15 cm across the fault 30 min after the event. Those observations demonstrate that rupture of the Superstition Hills fault was the primary cause of the 24 November event. Aftershock distribution verifies this interpretation (Magistrale et al., 1989). A first-motion focal mechanism of right-lateral strike slip on a vertical plane striking 305° (Magistrale et al., 1989) for the Superstition Hills earthquake is compatible with the strike and sense of slip of the Superstition Hills fault.

The M_s 6.2 Elmore Ranch earthquake preceded the Superstition Hills earthquake by 11 hr. This earlier event involved primarily left-lateral rupture of northeast-striking faults oriented perpendicular to the northern Superstition Hills fault (Fig. 1) (Hudnut et al., 1989; Sharp et al., 1989; Magistrale et al., 1989).

In the process of documenting displacement of the Superstition Hills fault associated with the Superstition Hills earthquake, it became apparent that afterslip was proceeding rapidly. We made repeated measurements of fault displacement in

EXPLANATION

ACTIVE FAULT ▬▬▬▬▬······
EAST BOUNDARY OF
CRYSTALLINE BASEMENT ······
BRAWLEY SEISMIC ZONE ▒▒▒▒▒

DEPTH TO 5.65 km /SEC
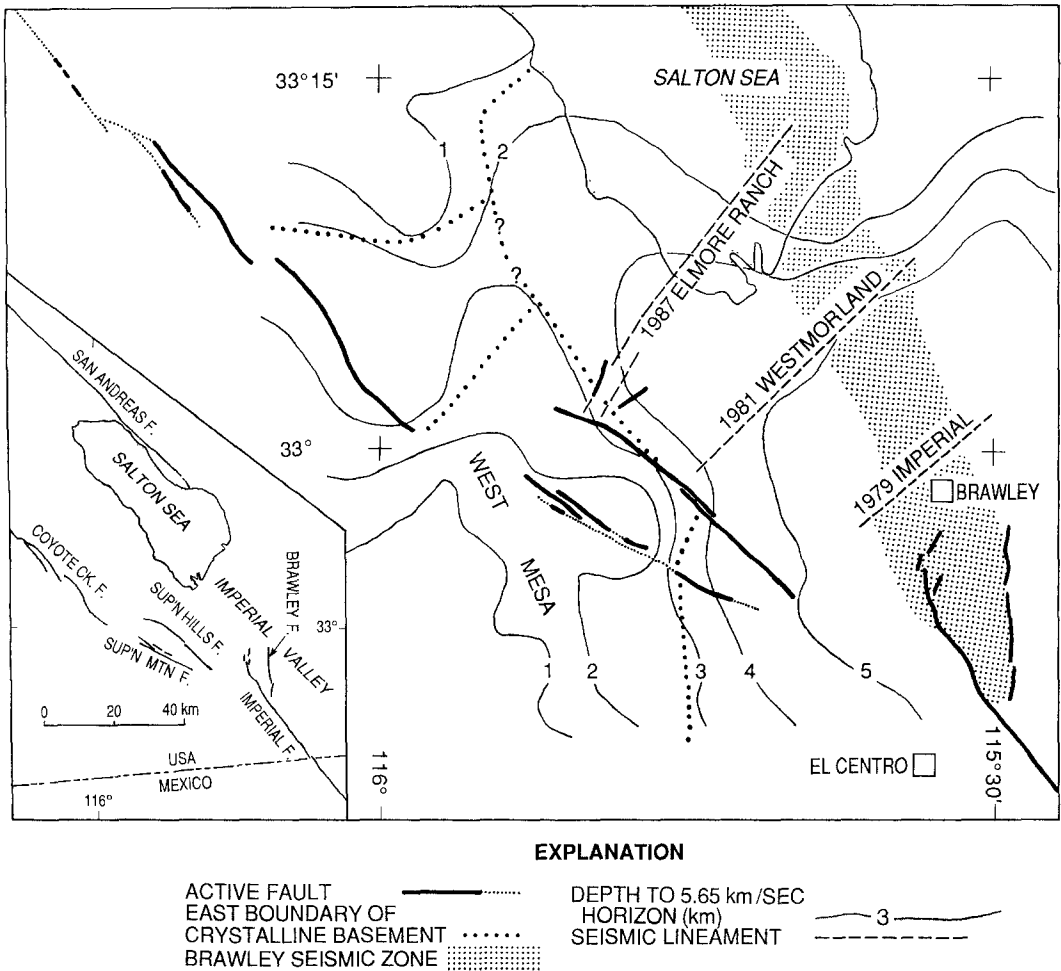 HORIZON (km)
SEISMIC LINEAMENT ─ ─ ─ ─ ─ ─

FIG. 1. Tectonic environment of the Superstition Hills fault. Shown in the inset are the Brawley, northern Imperial, and southern San Andreas faults. Branches of the southern San Jacinto fault zone, including the Coyote Creek, Superstition Mountain, and Superstition Hills faults, are also shown. Most fault locations are from Sharp (1982). Major northeast-trending seismic lineaments are dashed. These were expressed in association with the 1979 Imperial Valley (Johnson and Hutton, 1982), the 1981 Westmorland (Hutton and Johnson, 1981), and the 1987 Elmore Ranch earthquakes (Magistrale *et al.*, 1989). Contours correspond to depth in kilometers to the 5.65 km/sec seismic velocity associated by Kohler and Fuis (1986) with the base of unmetamorphosed sediments. The bold dotted line indicates the boundary of continental basement as inferred by Fuis and Kohler (1986). A basin in the area adjacent and east of the southern Coyote Creek fault was detected by analysis of residuals in earthquake locations obtained with portable stations (Hamilton, 1970) and by refraction methods (Kohler and Fuis, 1986).

order to attempt to discover relationships between afterslip parameters and the geological character of the fault. We correlate afterslip behavior to prominent geometric features of the fault trace including a bend and a right step, to a large increase in the thickness of sedimentary cover from north to south along the fault, and to the presence of buried continental crystalline basement along the fault's northern half.

Tectonic Setting

   The Superstition Hills fault is one of the prominent northwest-trending faults at the transition from the East Pacific Rise-Gulf of California spreading system to the southern California continental transform system. This fault appears to cut from

crust that lies within the extensional Gulf of California province to continental crust at the edge of the Peninsular Ranges province (Fuis *et al.*, 1982). Rupture of faults adjacent to the Superstition Hills fault caused a number of significant earthquakes during the past 20 yr. These include the 1968 rupture of the Coyote Creek fault (Clark, 1972), 1940 and 1979 ruptures of the Imperial fault (Richter, 1958; Sharp *et al.*, 1982), and the rupture of an unnamed northeast-striking fault in the 1981 Westmorland earthquake (Fig. 1) (Hutton and Johnson, 1981). Of the larger, mapped, active faults within the Salton trough, only the San Andreas and Superstition Mountain faults have not ruptured in the past 20 yr period (Fig. 1).

METHODS

We measured surface displacements along the 24 km length of the Superstition Hills fault at successive times, from 2 hr to 11 months after the 24 November 1987 Superstition Hills earthquake. During reconnaissance along two major segments of the fault rupture, many relatively simple sections of the fault were identified. These sections of the fault are single stranded and are locally parallel to the overall strike of the Superstition Hills fault. Most of our displacement measurements were made within these simple sections where a large fraction of surface displacement occurred across a narrow zone.

Initial Measurements

Determination of initial slip was accomplished by matching features across the fault (Fig. 2). Most of our measurements were made across small extensional fault jogs (Fig. 2b) and offset tire tracks (Fig. 2c). A few fresh and well-defined channel offsets were measured. These features allowed precise determination of right-lateral displacement parallel to the local strike of the fault. At some sites, several features were offset; in these cases measurements were combined for a mean site displacement. The uncertainty of most initial measurements was 5 mm. Each site was named (Fig. 3), and alignment marks were made across the fault by painting a 1- to 2-m-long reference line directly on the ground surface. Even on sandy surfaces the paint lines were durable for at least several weeks. This durability allowed accurate slip determinations after the original offset features eroded. Primary and successive slip measurements are necessarily small in aperture (i.e., 1 to 2 m) because initial offsets could be accurately determined only for discrete fractures.

Remeasurements

Many sites were revisited several times within 12 days of the earthquake. Our most comprehensive surveys were made on 25 November and 5 and 6 December 1987, and 25 and 26 January and 24 October 1988. On 24 November 1987, 14 sites were measured and marked with paint alignments. By 27 November 1987, 35 sites were established. These sites were remeasured and remonumented, and 18 additional sites were established on 5 and 6 December 1987. On 25 and 26 January 1988, 49 sites were remeasured and on 24 October 1988, 33 sites were remeasured. Additional measurements were made at intermediate and subsequent times at some very accessible sites.

During site visits, paint-line offsets were measured (Fig. 2d), remaining original offset features were measured, and more durable alignment monuments were established to replace deteriorated paint-lines. At most sites, linear arrays of nails were pushed into the soil and covered with stone cairns. Offsets were measured with the aid of two straight edges and a measuring tape. Uncertainty in these measure-
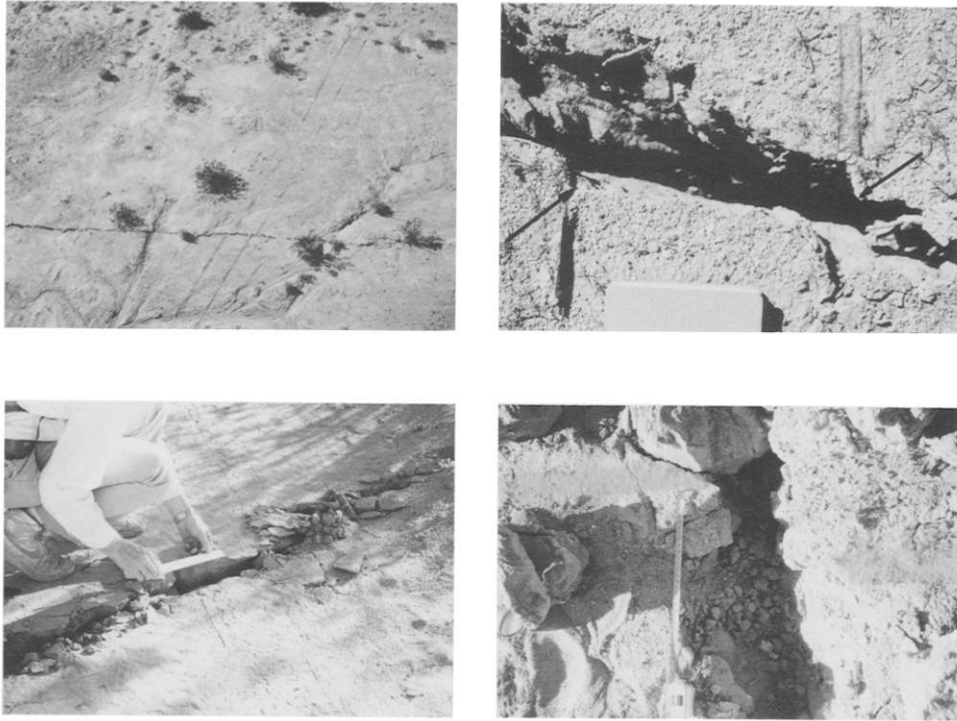
FIG. 2. Photos of offset features. Photo 2a: taken at about 1100 24 November 1987, an aerial view showing offset tire tracks and stream channels across the Superstition Hills fault. Photo 2b: arrows point to matching soil-crust features offset at site 1R. These features were used for most of the initial slip measurements. Photo 2c: offset tire tracks were used for initial slip measurement at site 2T. Photo 2d: at site 2U, a paint-line established on 25 November 1987 was offset 16 cm by 6 December 1987. A measuring tape is positioned parallel to the fault.
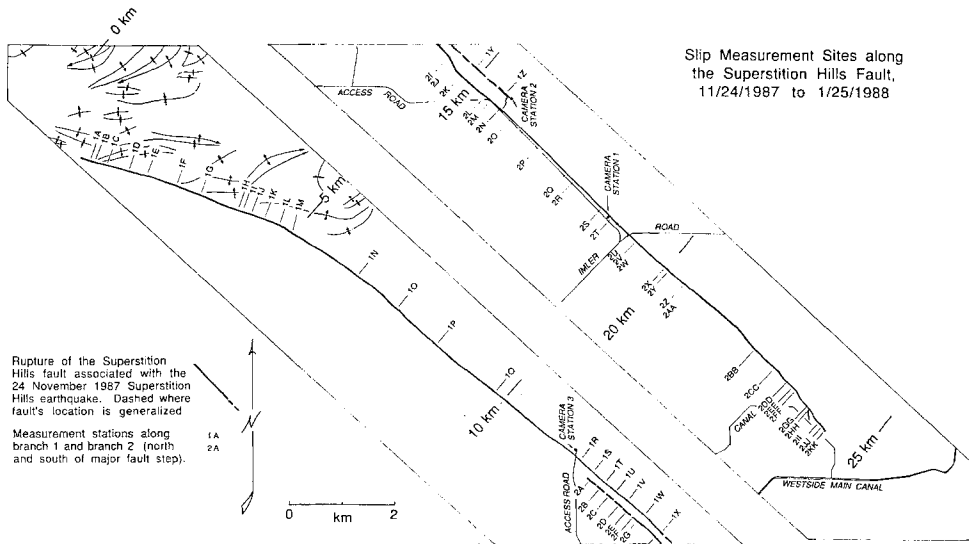
FIG. 3. Reference map of Superstition Hills fault and slip measurement sites. Sites are numbered from north to south. Sites along the northern segment are denoted 1A to 1Z, sites along the southern segment are denoted 2A to 2KK. Note the bend of the fault between km 4 and 5, and closely spaced tight folds in the Borrego Formation adjacent to the northern 6 km of the fault as mapped by Dibblee (1984). Folds in the same unit farther south along the fault are much more open. The zone of fault step-over, discussed in the text, is located between km 12.4 and 15.6.

ments was generally less than 3 mm, except at sites where substantial degradation of reference marks occurred.

<center>DATA</center>

Fault Segments

The fault is composed of two major segments (Fig. 3) that are distinguished by a right stepping zone of complex faulting. The northern and southern segments are approximately 14.9 and 12.1 km in length, respectively. These two segments overlap across a 3.5-km-long zone; thus, the rupture along the Superstition Hills fault was about 23.5 km in length, corresponding to the previously known extent of the fault. Sharp *et al.* (1989) have mapped ruptures that extend 3 km south of the previously known extent of the Superstition Hills fault. Slip across those ruptures is not described in this paper.

Character of Afterslip Accumulation

A sample of our afterslip data is presented in Figure 4. Our most complete records of fault slippage during the first 1800 hr period were acquired at sites about 6 km south of the mid-point of the Superstition Hills fault (sites 2T and 2U, Fig. 3). Displacement at site 2T was 28 cm at 2.75 hrs, 39 cm at 28 hrs, and 67.1 cm at 1829 hrs (about 11 weeks). Displacement at site 2U was 18.3 cm at 2.15 hrs, 31 cm at 27.5 hrs, and 60.8 cm at 1832 hrs. Slip measurements for all sites are presented in the Appendix.

Afterslip behavior during the initial 1800 hrs at 13 sites is summarized in Figure
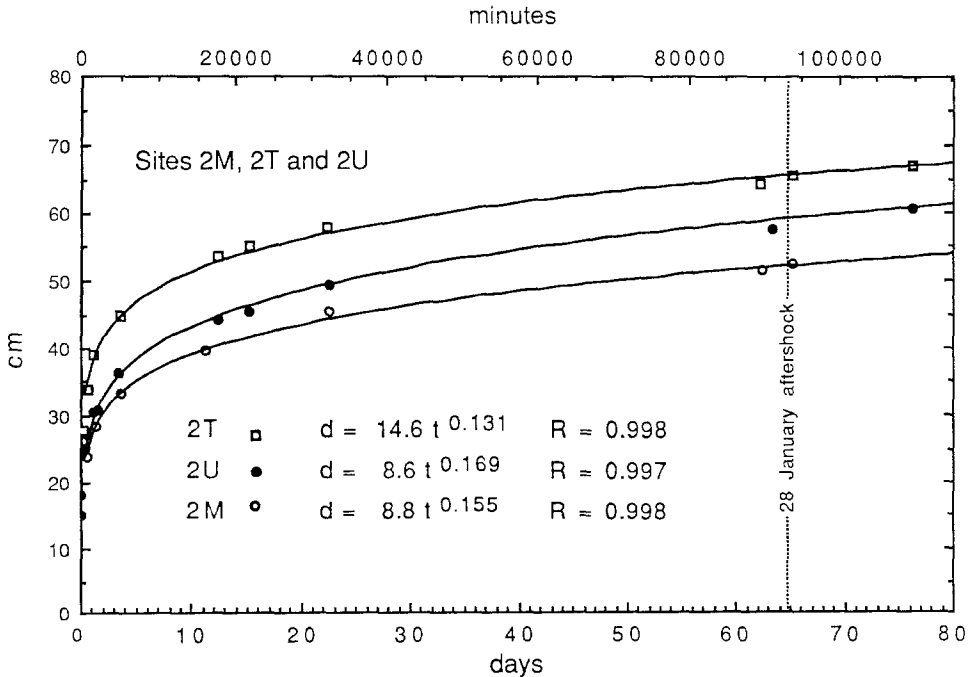

FIG. 4. Slip decay curves for sites 2M, 2T, and 2U. Note the increase of displacement at sites 2 M and 2T after a large aftershock (M_L 4.9) on the 28 January 1988. To the right of the key are power-law equations of the form, $d = at^b$ (b < 1), where d is displacement in cm, t is time in minutes, a and b are constants. Also listed is the correlation coefficient (R).

5. We find that these afterslip data display a decrease in rate that is well described by the power law

$$d = at^b \ (b < 1) \tag{1}$$

where d is displacement, t is time after the earthquake, a is a constant indicating displacement at $t = 1$, and b is a rate constant. The data plotted in Figure 5 are from sites that were initially measured between 2.15 and 35 hrs after the main shock. Very similar afterslip behavior was observed at sites 1P and 1Q, and at 2H, 2I, 2J, 2K, and 2M (locations shown in Fig. 3); in these cases, data from the single most completely described site are plotted. A larger number of sites for the southern segment reflects earlier investigation of that area.

The data summarized in Figure 5 are illustrated together with least-square regressions. Assuming constant power-law behavior throughout the initial 1800 hr period of earthquake afterslip, we estimate the slip at $t = 1$ min after the main shock origin time and its 95 per cent confidence interval, as shown in Figures 5a and 5 b. The 95 per cent confidence intervals are ±10 to 35 per cent of the inferred co-seismic slip for the northern segment and ±5.5 to 104 per cent along the southern segment.

Distribution of Slip Along the Fault

The spatial distribution of displacement at six intervals after the earthquake is illustrated in Figure 6. A high rate of afterslip is evident at some localities. Also apparent are some deviations from a simple distribution of slip along the fault. Two apparently anomalous features in Figure 6 are defined by several measurements. From the north, these are an abrupt step in the displacement profile at km 4.5, and a broad "saddle" in the profile between km 12.4 and 15.6.

DISCUSSION

Tectonic Features and Subsurface Geometry of the Imperial Valley

The Imperial Valley is a topographic expression of the Salton trough in south-eastern California. The trough formed by continental rifting at the northern tip of the Gulf of California (Lomnitz *et al.*, 1970; Elders *et al.*, 1972). Dominating the modern tectonic setting of the Salton trough is a through-going system of transform faults: the Imperial fault, the San Andreas fault, and southern branches of the San Jacinto fault system including the Superstition Hills, Superstition Mountain, and Coyote Creek faults (Fig. 1). Rupture of faults that define, or are near, the western margin of the Salton trough caused the 1987 Superstition Hills earthquake sequence.

Seismic refraction data indicate that sediment thickness in the Salton trough is greater than 4 to 5 km across most of the width of the Imperial Valley (Fig. 1) (Fuis *et al.*, 1982). Fuis *et al.* presented seismic velocity profiles within the valley showing a smooth increase of velocity to depths of about 5 km. Quite different velocity profiles were found in the "West Mesa" area, west of and adjacent to the Superstition Hills fault (Fig. 1). Those profiles show an abrupt increase of seismic velocity, to about 5.9 km/sec, at depths between 1 and 3 km. Kohler and Fuis (1986) interpreted the 5.9 km/sec horizon as the top of continental crystalline basement. These data indicate that continental crystalline basement is present beneath relatively thin sedimentary cover along the border of the western Salton trough. In addition Fuis

A

	key		A	B	R	CI
□	1U	$d =$	22.9 t	$^{0.099}$	1.000	10.0
+	1R	$d =$	17.3 t	$^{0.122}$	0.998	10.0
o	1Q	$d =$	18.2 t	$^{0.108}$	0.998	12.0
✻	1O	$d =$	14.3 t	$^{0.102}$	0.999	35.0
▣	1G	$d =$	5.3 t	$^{0.103}$	0.999	14.0

B

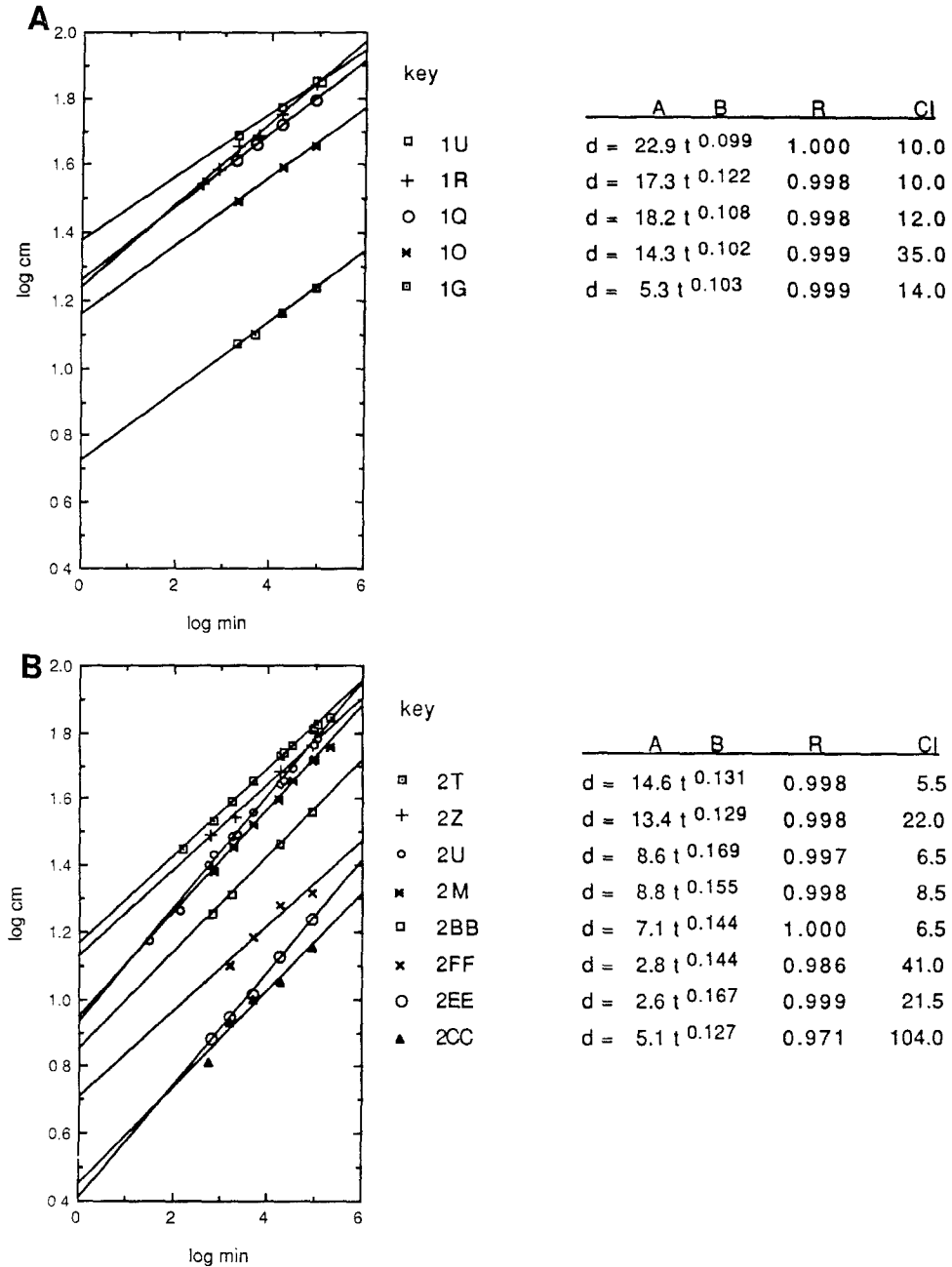|	key		A	B	R	CI
□	2T	$d =$	14.6 t	$^{0.131}$	0.998	5.5
+	2Z	$d =$	13.4 t	$^{0.129}$	0.998	22.0
o	2U	$d =$	8.6 t	$^{0.169}$	0.997	6.5
✻	2M	$d =$	8.8 t	$^{0.155}$	0.998	8.5
□	2BB	$d =$	7.1 t	$^{0.144}$	1.000	6.5
×	2FF	$d =$	2.8 t	$^{0.144}$	0.986	41.0
○	2EE	$d =$	2.6 t	$^{0.167}$	0.999	21.5
▲	2CC	$d =$	5.1 t	$^{0.127}$	0.971	104.0

FIG. 5. Logarithmic plots of slippage along the Superstition Hills fault. Part a and b show data from five sites along the northern fault segment, and eight sites along the southern segment, respectively. The first measurement at site 2U was made by Kahle *et al.* (1988). Power-law equations and correlation coefficients are listed to the right as in Figure 4. The 95 per cent confidence interval (CI) cited is a percentage of slip at $t = 1$ min; e.g., at site 1U there is 95 per cent confidence that the displacement at $t = 1$ min was 22.9 ± 10 per cent (22.9 ± 2.3 cm).

et al. (1982) suggested that continental basement is absent within the Salton trough itself, and that metasedimentary rocks dominate at depths from 5.5 to 13 km.

Major basement surfaces in the vicinity of the Superstition Hills fault, at depths of about 1.5, 2.5, and 4.5 km (Kohler and Fuis, 1986), are interpreted by Fuis *et al.*
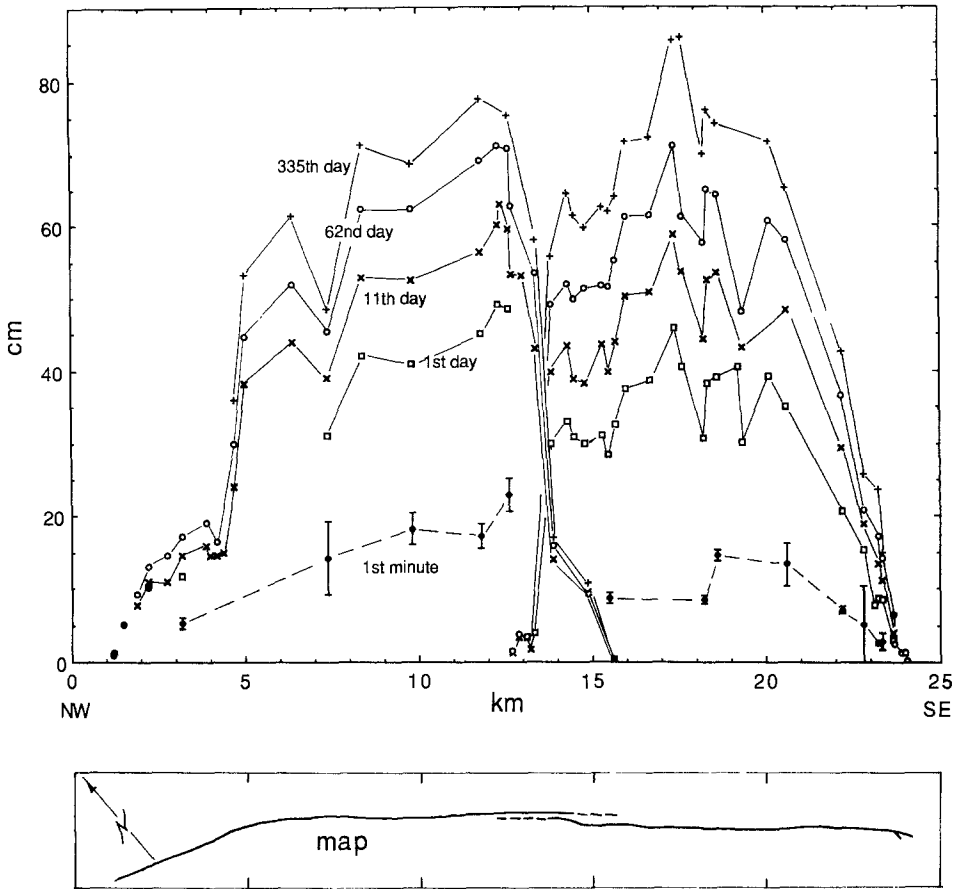
FIG. 6. Afterslip plotted along the fault. The illustrated displacements were observed on 25 November and 5 and 6 December 1987, and on 25 January and 24 October 1988. Solid dots illustrate measurements of the northern extent of the surface rupture made on 27 November 1987. Dashed lines connect displacements inferred at $t = 1$ min after the main shock in Figures 5a and b. Error bars show 95 per cent confidence intervals for these points. The fault is plotted in map view below. Note that the fault is composite of two segments and that smaller displacements occurred where the segments overlap. Note also the sudden increase in slip near the abrupt fault bend about 5 km from the northeast end of the fault. These features are discussed in the text.

(1982) to represent down-faulted basement blocks at the western edge of the Salton trough. The Superstition Hills fault appears to bound and to cut an escarpment defining the eastern boundary of the 2.5-km-deep basement surface (Fig. 1).

Association of Slip Distribution with Surficial Geometry of the Fault

Displacement of the Superstition Hills fault correlates with the fault's geometry. Two distinctive departures from a simple elliptically-shaped along-fault displacement profile occur at a bend and a step that define boundaries of fault segments. At km 4.5 (Fig. 6) an 18° fault bend is associated with an abrupt increase of slip magnitude to the south. The more westerly striking part of the fault to the north cuts through a zone of uplifted and closely folded Pleistocene strata of the Borrego Formation (Fig. 3). Geologic mapping of this area by Dibblee (1984) indicates the Plio-Pleistocene strata are much more tightly folded near the northernmost Superstition Hills fault than elsewhere along the fault. Displacement in this area is

presumably taken up in local folding of the Borrego Formation or in uplift of the whole of the northern Superstition Hills area (Fig. 1).

The M_s 6.2 rupture of left-lateral faults that are located northeast of, and strike perpendicular to, the northern Superstition Hills fault occurred just 12 hrs prior to the Superstition Hills earthquake (Fig. 1) (Magistrale et al., 1989); this event suggests a second candidate for causing the abrupt increase of slip observed at km 4.5. Presumably, movement of several left-lateral fault strands in the 23 November earthquake produced higher normal stresses across the Superstition Hills fault northwest of the intersection of the right- and left-lateral faults. If normal stress across the Superstition Hills fault were reset by the earlier event (Given and Stuart, 1988; Hudnut et al., 1989), displacement in the subsequent Superstition Hills earthquake may have been locally impeded. Because the zone of intersecting left-lateral faults is widely distributed and located northwest of the prominent step in the slip profile (Hudnut et al., 1989; Sharp et al., 1989), it is probable that the 18° bend of the Superstition Hills fault, not the action of intersecting left-lateral faults, principally caused the abrupt change in slip magnitude at km 4.5.

A "saddle" in the slip profile is associated with a 3.5-km-long zone where fault segments extending from the north and south overlap (km 12.4 to 15.6, Fig. 6). Slip must be transferred between the overlapping faults in this zone. Locally within this zone, the magnitude of slip accounted for by summing slip across adjacent sites on the two main strands is close to the maxima outside the area of the right step and so the decrease of observed slip is only apparent. The efficiency of slip transfer between the two echelon strands may be due to the step's "releasing" geometry. We note that the position of this segment boundary corresponds to the projection of a prominent lineation defined by aftershocks of the 1981 Westmorland earthquake (Hutton and Johnson, 1981) and is near to a steep subsurface escarpment at the edge of continental crystalline basement rocks between the Superstition Hills and Superstition Mountain faults (Fuis and Kohler, 1986; Kohler and Fuis, 1986) (Fig. 1). We suggest that fault complexity in the right-stepping zone probably reflects the location of a major boundary between basement blocks beneath the step.

Creep across the Superstition Hills fault in 1968, 1979, and 1981 was triggered by local earthquakes (Allen et al., 1972; Fuis, 1982; Sharp et al., 1986). The location of 1987 surface rupture corresponds closely to the mapped trace of the recent aseismic displacements. Some details of the 1987 rupture pattern, however, were not observed in earlier triggered aseismic slip events. Surface fractures associated with the 1968 and 1979 events were mapped continuously through a prominent bend and the northern and southern branches of the fault were connected (Fig. 3). This suggests that the earlier aseismic ruptures were much less complicated than the rupture pattern associated with the 1987 earthquake.

Association of Afterslip Behavior with Subsurface Geology

An abrupt change in afterslip behavior near km 13 (Fig. 3) correlates with the boundary of the two overlapping fault segments discussed earlier, to large increase in the thickness of sedimentary rock southeastward, and to a marked boundary of basement rock type (Fig. 1). The northern segment of the Superstition Hills fault experienced a significantly smaller amount of afterslip than the southern segment during the time periods 30 to 280 hrs and 30 to 1500 hrs after the Superstition Hills shock. The percentage increase of afterslip is compared in Figure 7 between field
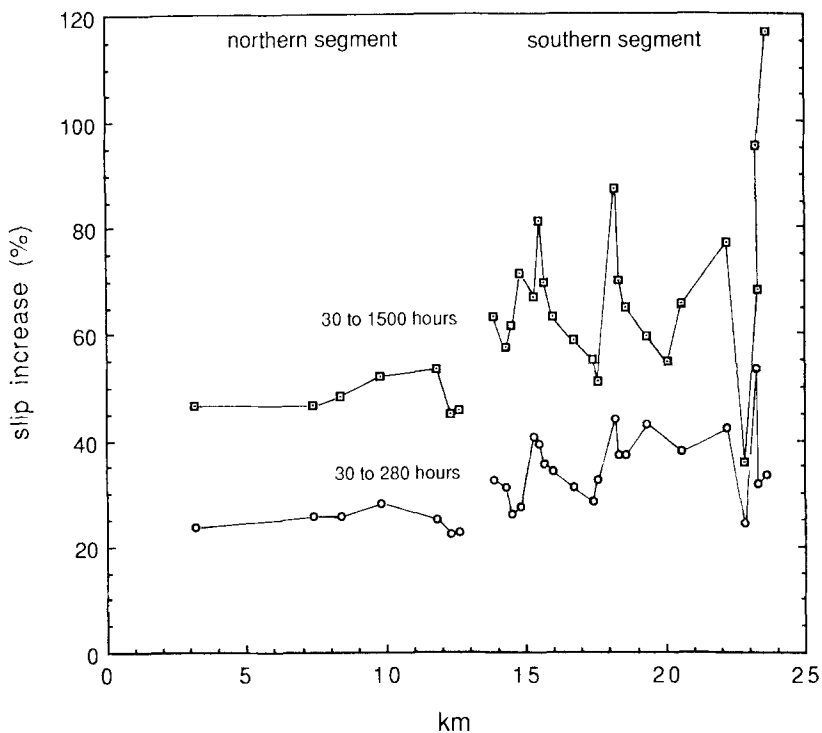
FIG. 7. The percentage increase in afterslip between field measurements made 30 ± 5, 283 ± 17, and 1505 ± 15 hrs after the earthquake. The increase of slip from 30 to 280 hrs was 24.5 ± 2 per cent and 35.5 ± 7 per cent along the northern and southern branches of the fault, respectively. Between 30 and 1505 hr, the slip increased 48 ± 3 per cent along the northern segment of the fault and 69 ± 10.5 per cent along the southern segment.

measurements made 30 ± 5, 283 ± 17, and 1505 ± 15 hrs after the earthquake. The increase of slip from 30 to 280 hrs is 24.5 ± 2 per cent (1 S.D.), along the northern segment of the fault and 35.5 ± 7 per cent along the southern segment. Between 30 and 1505 hrs, slip increased 48 ± 3 per cent along the northern segment of the fault and 69 ± 10.5 per cent along the southern segment (Fig. 7). (The high and low points along the southern segment for the 30 to 1500 hour period were maxima and minima for this time period. Because they appear to be anomalous, they are not considered in calculating uncertainty.) Total displacement along the two fault segments is similar, this result suggests that a greater proportion of co-seismic slip or early aseismic slip occurred along the northern segment (Fig. 6).

Although the slip increase cited for the northern segment is defined by only seven data points, behavior is clearly more uniform there than that along the southern segment. This indicates that factors controlling the magnitude of co-seismic slip and rate of afterslip must be relatively consistent along the northern segment. We speculate that the presence of a large block of continental crystalline basement buried at relatively uniform depth along the northern segment moderated slip behavior there. This idea is suggested by the location crystalline basement proposed by Fuis et al. (1982) and Fuis and Kohler (1986).

The depth of young sedimentary cover and the geometry of buried basement blocks along the boundary of Salton trough appear to have strongly influenced the

slip behavior of different segments of the Superstition Hills fault. The northern segment appears to have experienced larger co-seismic, or early aseismic slip, than the southern segment, but the mean rate of slip was significantly larger across the southern segment between 30 and 1500 hrs after initial rupture. According Fuis *et al.* (1982) and Kohler and Fuis (1986), 2.5 and 3.5 km of young sedimentary cover overlies old continental basement along the northern Superstition Hills fault, but at least 4 to 5 km of sedimentary cover overlies metasedimentary rock along the southern part of the fault. The presence of shallow continental basement and thinner sedimentary cover are thus correlated with larger early, probably co-seismic displacement of the northern branch of the fault. Reciprocally, a greater depth to basement and substantially thicker sedimentary cover are correlated with smaller co-seismic (or early aseismic) displacements and to more rapid aseismic surficial slip over the first several days of the postseismic period. Substantially different behavior of the northern and southern fault segments is further supported by the observation of Magistrale *et al.* (1989) that aftershocks during the 4 days following the main shock were densely clustered along the northern Superstition Hills fault segment, but were sparse and were generally smaller in magnitude along the southern segment.

In reviewing afterslip distributions associated with some earlier, well-described strike-slip earthquakes, we find that the geometry of basement rocks, and sediment thickness appear to play roles in the distribution of net surface displacement between co-seismic and aseismic processes. Slip behavior along the three Coyote Creek fault segments that ruptured in association with the April 1968 Borrego Mountain earthquake was closely correlated to the depth of basement rocks and sedimentary thickness. Continental basement rocks are present at depths of 0 to 1000 m on both sides of the northern 13 km of the 1968 rupture (Hamilton, 1970; Fuis *et al.*, 1982). Almost no afterslip was detected along this segment (Clark, 1972). An increase of fault slip between 25 to 800 per cent occurred aseismically during the initial 3 month postseismic period along the central and southern segments of the fault (Clark, 1972). Burford (1972) correlated the large afterslip observed along the central Coyote Creek fault segment to the depth of sedimentary strata in that area (up to 3.5 km, Hamilton, 1970; Kohler and Fuis, 1986). Fuis *et al.* (1982) suggested that continental basement may be absent on the northeast side of the southern Coyote Creek fault segment (Fig. 1). Although refraction data are too sparse to distinguish unambiguously the presence or absence of buried continental crystalline basement there (G. S. Fuis, personal comm., 1988), the results of Hamilton (1970) and Kohler and Fuis (1986) both indicate the presence of an at least 3 to 3.5 km thickness of sedimentary cover northeast of the southern Coyote Creek fault (Fig. 1). The occurrence of large amounts of afterslip was thus confined to sections of the Coyote Creek fault where continental basement rocks are juxtaposed against an at least 3.5 km thickness of young sedimentary rock across the fault. We thus concur with Burford (1972) that boundaries between zones of differing slip behavior were probably controlled by sediment thickness in the 1968 rupture and propose that such a relationship also held for the 1987 Superstition Hills rupture.

Supporting this idea are observations of afterslip behavior along the 1979 Imperial fault surface rupture (Sharp *et al.*, 1982) (Fig. 8). The Imperial fault cuts a homogeneous stratigraphic section consisting of a 5 km thickness of young sedimentary rocks overlying metasedimentary rocks (Fuis *et al.*, 1982). Unlike the 1968 and 1987 ruptures, abrupt changes of slip behavior were not detected along the 1979
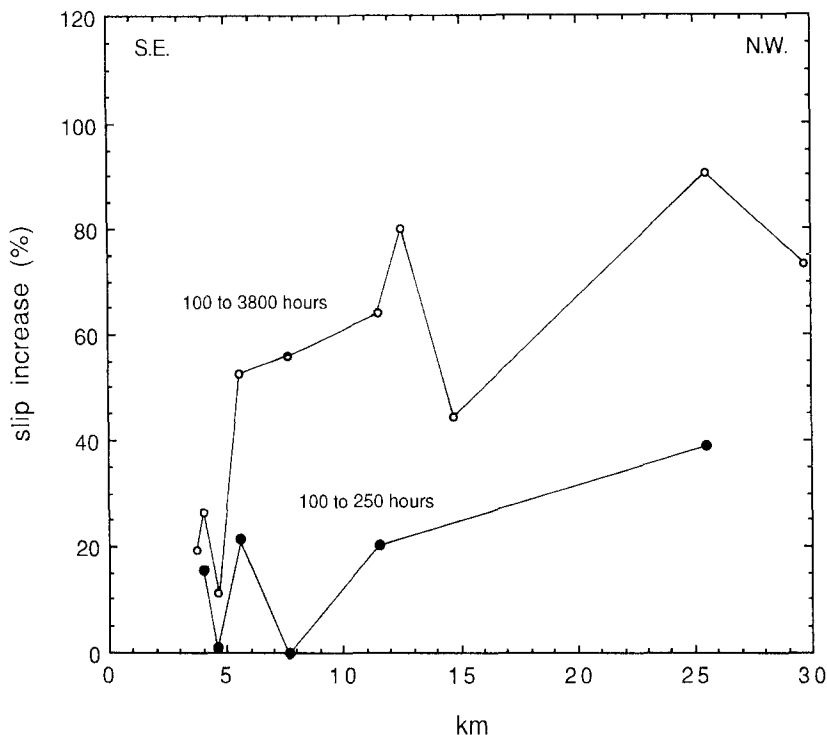
FIG. 8. The percentage increase of slip between 4 and 10 days and 4 and 160 days after the Imperial Valley earthquake as measured by Sharp *et al.* (1982).

Imperial fault rupture. We suggest that afterslip behavior observed after the 1979 event is consistent with small variation of sediment thickness along the Imperial fault.

The occurrence of aseismic surficial fault displacement in areas with substantial accumulations of poorly consolidated sediment indicates the existence of a physical mechanism for velocity strengthening of poorly consolidated sedimentary rock (Marone and Scholz, 1988; Scholz, 1989). Marone and Scholz presented experimental data showing velocity strengthening in poorly consolidated granular quartz. They argue that aseismic surficial slip results from velocity strengthening in poorly consolidated fault gauge. This mechanism is plausible for aseismic afterslip of the Superstition Hills fault where, as has been described, young sedimentary rock extends to several kilometers depth.

That aseismic slip appears to have a larger contribution to total displacement where young sedimentary cover is deeper along the Superstition Hills fault suggests that magnitudes of co-seismic slip and afterslip are in part a function of the thickness of poorly consolidated material overlying a fault.

Did Co-seismic Surface Slippage Occur Along the Superstition Hills Fault?

For convenience we define co-seismic slip as displacement that occurred during the first minute after the main-shock origin time. Although no primary observations or records demonstrate that co-seismic slip occurred at the surface along the Superstition Hills fault, the power-law fit of the repeated measurements of subsequent aseismic slip (Figs. 5a, b) suggest that as much as 23 cm of co-seismic surface slip occurred (Fig. 6).

Apparently no significant slip of the Superstition Hills fault occurred prior to the 24 November earthquake. A creepmeter at Camera Station 2 (Fig. 3) recorded no slip between 12 January and 27 October 1987 (McGill *et al.*, 1989), and no observable surface displacement had occurred at Imler Road (site 2U) as of 2.5 hr before the earthquake (Kahle *et al.*, 1988). On the other hand, Kahle *et al.* observed 15 cm of dextral slippage at Imler Road 30 min after the main shock, and slip of 18.3 cm had occurred at this site 2.15 hrs after the event (this study).

Power-Law Slip Behavior

Afterslip described by a simple logarithmic law was documented in association with the Parkfield, Borrego Mountain, and Imperial Valley, California, earthquakes (Scholz *et al.*, 1969; Burford, 1972; Cohn *et al.*, 1982). In marked contrast, slip of the Superstition Hills fault associated with the 1987 earthquake followed a power law during the first several-hundred-hour postseismic period.

Plotted on Figure 5 are several least-square regressions to afterslip data. The regressions indicate that equations of the power-law form successfully describe the initial several hundred hours of postseismic slip data. The validity of these regressions is supported by a 15 cm displacement measured 30 min after the earthquate by Kahle *et al.* (1988). That point, measured at site 2U, is plotted in Figure 5b. It plots precisely on the site 2U regression line.

The afterslip data presented in Figure 5 are not well described by logarithmic functions in time. Slip at early times was much larger than indicated by logarithmic regression lines (Fig. 9). The first dextral offset measured after the earthquake. at site 2U (Kahle *et al.*, 1988), is several centimeters larger than inferred by logarithmic regression of data collected over the subsequent weeks. In addition, collective plots of these data retain a concave upward nonlinearity when plotted on semi-log
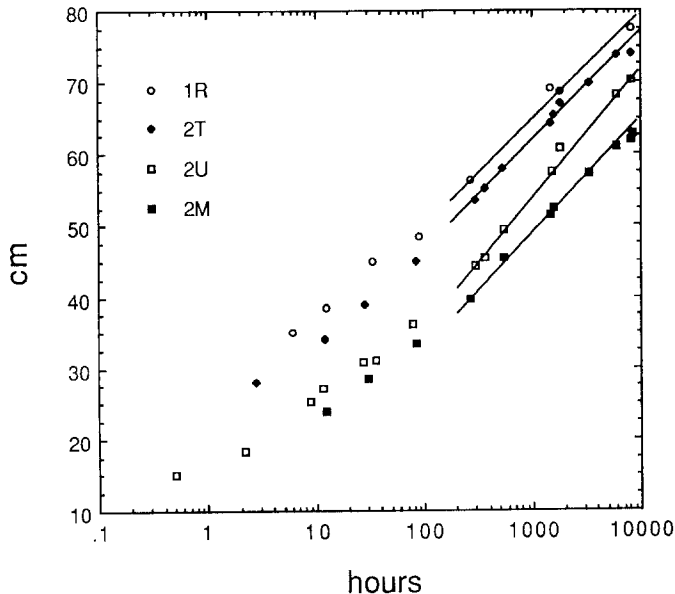
FIG. 9. Displacements at sites 1R, 2M, 2T, and 2U (Fig. 3) between 0 and 335 days after the Superstition Hills earthquake plotted in a semi-log field. Measurements made 2 weeks to 335 days after the event are relatively well described by a logarithmic function, as shown by straight-line fits to those data. Measurements made within the first 2 weeks do not fit the later log trend and are better fit by a power law as illustrated in Figs. 4 and 5.

coordinates (Fig. 9). An unacceptable result of the logarithmic regression is the inference that most fault displacements at $t = 1$ min were significantly less than zero.

Some of the small deviations of individual measurements from the general form of the power-law decay curves (Figs. 4 and 5) must partly result from the intermittent occurrence of slip episodes in which several millimeters of slip occur (Bilham, 1989). In addition, the occurrence of slip at sites 2M and 2T between 26 and 28 January 1988 (Fig. 4) was probably associated with a large aftershock (M_L 4.9) at 0254 GMT on 28 January 1988. Significant retardation of afterslip at three sites was observed shortly before the aftershock. Remeasurement at two of these sites within a few hours after the aftershock suggests that ground shaking triggered rapid slippage of the fault and total displacement stepped abruptly up to the trend of measurements at earlier and subsequent times.

Wesson (1988) investigated the dynamics of aseismic fault slippage. He modeled afterslip of the 1966 Parkfield and 1979 Imperial Valley earthquakes as the response of several aseismically slipping strips to a deeper, instantaneous, brittle rupture. The model utilized a quasi-plastic rheology in the aseismically slipping layers and assumes zero external stress on the fault plane and zero co-seismic slip at the surface. This model successfully fits the observations of afterslip in the 1966 and 1979 earthquakes, except at small times (Fig. 9 in Wesson, 1988). The afterslip data fit by Wesson's model can be described by a simple function of the form:

$$d = a + b \log t \tag{2}$$

where d is surface displacement, t is time after co-seismic rupture, and a and b are constants. Wesson suggests that poor fit at small times may be due to the neglect of co-seismic slip, which would require a more complex rheology in his model. We observe power-law decay of afterslip at small times, and given Wesson's success at modeling log decay, we suggest that at short times external stress may be a significant factor in driving the observed surface slip.

Projected Total Surface Displacement

The afterslip data invite predictions of the course of fault displacement over the coming months and years. We reviewed slip data measured across the Imperial fault subsequent to the 1979 Imperial Valley earthquake as reported by Cohn *et al.* (1982) and Louie *et al.* (1985) and from C. R. Allen, (personal comm., 1988). These data demonstrate continuing logarithmic increase in afterslip between 18 hrs and 8 yrs after that event. The slippage is described by simple logarithmic functions of the form shown in equation (2). While the Superstition Hills afterslip data from the initial few hundred hour period are poorly fit by this equation, as discussed earlier, behavior subsequent to this is well described by the simple logarithmic expression. This suggests that over long periods afterslip follows a logarithmic form as was formerly suggested. Assuming continuation of the current logarithmic behavior at sites 1R, 2M, 2T, and 2U (Fig. 9), in 10 yrs displacements there will approach about 93, 78, 91, and 90 cm, respectively. These displacements are consistent with estimates of co-seismic displacement at seismogenic depths as inferred from regional geodetic data (Lisowski and Savage, 1988) and as can be deduced from the moment estimates of Bent *et al.* (1989). In addition, we note that projected slip over a 10 yr period across the 150-m-wide Caltech alignment array (400 m south of site 2T) is

just 5 cm greater than that suggested by extrapolation of current logarithmic behavior at site 2T (McGill *et al.*, 1989).

CONCLUSIONS

We find that afterslip displacement along the Superstition Hills fault has been predictable during the period of this study, and that it is well described by a power law, $d = at^b$ (b < 1), during the initial several weeks after the main shock (d is displacement, t is time after the earthquake, and a and b are constants). Regression of power-law functions to $t = 1$ min after the earthquake suggests that up to about 23 cm of surface slippage along the Superstition Hills fault occurred co-seismically.

Most sites that were monitored during the 280 to 8000 hr postseismic interval exhibit slip behavior that is well described by simple logarithmic function, $d = a + b \log t$. The apparent change of behavior from power-law to logarithmic slip decay is not explained. We note, however, that simple logarithmic behavior has been observed for the 9 yrs following the nearby Imperial fault rupture of 1979, and is thus precedented. Extrapolation of logarithmic fits to the data collected up to October 1988 suggest that displacement will reach about 90 cm by November of 1997, 10 yrs after the rupture.

The geometry of the Superstition Hills fault correlates well to details of the earthquake slip profile. Toward the northwest end of the fault slip decreased abruptly at a prominent fault bend that is associated with uplift and tight folding of sedimentary rocks. Change of slip magnitude is also observed at a major right step near the center of the fault.

Afterslip behavior correlates well with subsurface geology as interpreted from seismic refraction studies. A relatively larger percentage of afterslip appears to have occurred where the fault cuts a thicker section of late Cenozoic sedimentary strata; we also observe that more uniform afterslip behavior occurred where the fault cuts continental crystalline basement. Change in slip behavior along the fault thus appears to be strongly dependent on the constitutive properties of rocks bounding the fault.

REFERENCES

Allen, C. R., M. Wyss, J. N Brune, A. Granz, and R. Wallace (1972). Displacements on the Imperial, Superstition Hills, and San Andreas faults triggered by the Borrego Mountain earthquake, in *The Borrego Mountain Earthquake, U.S. Geol. Surv. Profess. Paper 787*, 87–104.

Bent, A. L., D. V. Helmberger, R. J. Stead, and P. Ho-Liu (1989). Waveform modelling of the November 1987 Superstition Hills earthquakes, *Bull. Seism. Soc. Am.* **79**, 500–514.

Bilham, R. G. (1989). Surface slip subsequent to the 24 November 1987 Superstition Hills earthquake, California, monitored by digital creepmeters, *Bull. Seism. Soc. Am.* **79**, 424–450.

Burford, R. O. (1972). Continued slip of the Coyote Creek fault after the Borrego Mountain earthquake, in *The Borrego Mountain Earthquake, U.S. Geol. Surv. Profess. Paper 787*, 105–111.

Clark, M. M. (1972). Surface rupture along the Coyote Creek fault, in *The Borrego Mountain Earthquake, U.S. Geol. Surv. Profess. Paper 787*, 55–86.

Cohn, S. N., C. R. Allen, R. Gilman, and N. R. Goulty (1982). Preearthquake and postearthquake creep in the Imperial fault and the Brawley fault zone, in *The Imperial Valley Earthquake of October 15, 1979, U.S. Geol. Surv. Profess. Paper 1254*, 161–167.

Dibblee, T. W., Jr. (1984) Stratigraphy and tectonics of the San Felipe Hills, Borrego Badlands, Superstition Hills, and vicinity, in *The Imperial Basin—Tectonics Sedimentation and Thermal Aspects*, C. A. Rigsby (Editor), Pacific Section SEPM, Los Angeles 31–44.

Elders, W. A., R. W. Rex, T. Meidav, P. T. Robinson, and S. Biehler (1972). Crustal spreading in southern California, Science **178**, 15–24.

Fuis, G. S. (1982). Displacement on the Superstition Hills fault triggered by the earthquake, in *The Imperial Valley Earthquake of October 15, 1979, U.S. Geol. Surv. Profess. Paper 1254*, 145–154.

Fuis, G. S. and W. M. Kohler (1986). Crustal structure and tectonism of the Imperial Valley region, California, in *The Imperial Basin—Tectonics, Sedimentation and Thermal Aspects*, C. A. Rigsby (Editor), SEPM, Los Angeles, 1–13.

Fuis, G. S., W. D. Mooney, J. H. Healey, G. A. McMechan, and W. J. Lutter (1982). Crustal structure of the Imperial Valley region, in *The Imperial Valley Earthquake of October 15, 1979, U.S. Geol. Surv. Profess. Paper 1254*, 25–50.

Given, D. D. and W. D. Stuart (1988). A fault interaction model for triggering of the Superstition Hills earthquake of November 24, 1987 (abstract), *Seism. Res. Lett.* **59**, 48.

Hamilton, R. M. (1970). Time term analysis of explosion data from the vicinity of the Borrego Mountain earthquake of 9 April 1988, *Bull. Seism. Soc. Am.* **60**, 367–381.

Hudnut, K., L. Seeber, T. Rockwell, J. Goodmacher, R. Klinger, S. Lindvall, and R. McElwain (1989). Surface ruptures on cross-faults in the 23 November, 1987 Elmore Ranch earthquake, *Bull. Seism. Soc. Am.* **79**, 330–341.

Hutton, L. K. and C. E. Johnson (1981). Preliminary study of the Westmorland earthquake swarm (abstract), *EOS* **62**, 957.

Johnson, C. E. and L. K. Hutton (1982). Aftershocks and pre-earthquake seismicity, in *The Imperial Valley Earthquake of October 15, 1979, U.S. Geol. Surv. Profess. Paper 1254*, 59–76.

Kahle, J. E., C. J. Wills, E. W. Hart, J. A. Treiman, R. B. Greenwood, and R. S. Kaumeyer (1988). Preliminary report, surface rupture, Superstition Hills earthquakes of November 23 and 24, 1987, *California Geology* **41**, 75–84.

Kohler, W. M. and G. S. Fuis (1986). Travel-time, time-term, and basement depth maps for the Imperial Valley Region, California, from explosions. *Bull. Seism. Soc. Am.* **76**, 1289–1303.

Lisouski, M. and J. C. Savage (1988). Deformation associated with the Superstition Hills, California, earthquakes of November 1987 (abstract), *Seism, Res. Lett.* **59**, 35.

Lomnitz, C., F. Mooser, C. R. Allen, J. N. Brune, and W. Thatcher (1970). Seismicity and tectonics of the northern Gulf of California region, Mexico: preliminary results, *Geofísica Internacional* **10**, 37–48.

Louie, J. N., C. R. Allen, D. C. Johnson, P. C. Haase, and S. N. Cohn (1985). Fault slip in southern California, *Bull. Seism. Soc. Am.* **75**, 811–833.

Magistrale, H., L. Jones, and H. Kanamori (1989). The Superstition Hills, California, earthquakes of 24 November 1987, *Bull. Seism. Soc. Am* **79**, 239–251.

Marone, C. and C. H. Scholz (1988). The depth of seismic faulting and the upper transition from stable to unstable slip regimes. *Geophys. Res. Lett.* **15**, 621–624.

McGill, S. F., C. R. Allen, K. W. Hudnut, D. C. Johnson, W. F. Miller, and K. E. Sieh (1989). Slip on the Superstition Hills fault and on nearby faults associated with the 24 November 1987 Elmore Ranch and Superstition Hills earthquakes, southern California, *Bull. Seism Soc. Am.* **79**, 362–375.

Richter, C. F. (1958). *Elementary Seismology*, W. H. Freeman, San Francisco, 768 pp.

Scholz, C. H. (1989). *The Mechanics of Earthquakes and Faulting*, Cambridge University Press, New York (in press).

Scholz, C. H., M. Wyss, and S. W. Smith (1969). Seismic and aseismic slip on the San Andreas fault, *J. Geophys. Res.* **74**, 2049–2069.

Sharp, R. V. (1982). Tectonic setting of the Imperial Valley region, in *The Imperial Valley Earthquake of October 15, 1979, U.S. Geol. Surv. Profess. Paper 1254*, 5–14.

Sharp, R. V., J. J. Lienkaemper, M. G. Bonilla, D. B. Burke, B. F. Fox, D. G. Herd, D. M. Miller, D. M. Morton, D. J. Ponti, M. J. Rymer, J. C. Tinsley, J. C. Yount, J. E. Kahle, E. W. Hart, and K. E. Sieh (1982). Surface faulting in the central Imperial Valley, in *The Imperial Valley Earthquake of October 15, 1979, U.S. Geol. Surv. Profess. Paper 1254*, 119–144.

Sharp, R. V., M. J. Rymer, and J. J. Lienkaemper (1986). Surface displacements on the Imperial and Superstition Hills faults triggered by the Westmorland, California, earthquake of 26 April 1981, *Bull. Seism. Soc. Am.* **76**, 949–965.

Sharp, R. V., K. E. Budding, J. Boatwright, M. J. Ader, M. G. Bonilla, M. M. Clark, T. E. Fumal, K. K. Harms, J. J. Lienkaemper, D. M. Morton, B. J. O'Neill, C. L. Ostergren, D. J. Ponti, M. J. Rymer, J. L. Saxton, and J. D. Sims (1989). Surface faulting along the Superstition Hills fault zone and nearby faults associated with the earthquakes of 24 November 1987, *Bull. Seism. Soc. Am.* **79,** 252–281.

Wesson, R. L. (1988). Dynamics of fault creep, *J. Geophys. Res.* **93,** 8929–8951.

DIVISION OF GEOLOGICAL AND PLANETARY SCIENCES 170-25
CALIFORNIA INSTITUTE OF TECHNOLOGY
PASADENA, CALIFORNIA 91125

TABLE 1

APPENDIX

Site	Date	Time (PST)	Disp. (CM)	KM	Uncert. (CM)
1A	11/27/87	1500	1.0	1.20	0.25
1B	11/27/87	1500	1.3	1.25	0.25
1C	11/27/87	1430	5.1	1.50	0.25
1D	12/6/87	1325	7.8	1.90	0.25
	1/26/88	1503	9.3		0.25
1E	11/27/87	1400	10.3	2.25	0.50
	12/6/87	1310	11.1		0.20
	1/26/88	1452	13.1		0.15
1F	12/6/87	1252	11.0	2.75	0.25
	1/26/88	1442	14.6		0.25
1G	11/25/87	1617	11.8	3.20	0.25
	11/27/87	1320	12.6		0.20
	12/6/87	1130	14.6		0.20
	1/26/88	1335	17.3		0.20
1H	12/6/87	1145	16.0	3.90	0.25
	1/26/88	1411	19.1		0.25
1I	12/6/87	1225	14.5	4.00	0.50
1J	12/6/87	1200	14.5	4.20	1.50
	1/26/88	1408	16.5		1.50
1K	12/6/87	1210	15.0	4.40	2.5
1L	12/6/87	1055	24.0	4.70	0.25
	1/25/88	1700	30.0		0.25
	10/24/88	1700	36.0		0.5
1M	12/6/87	1003	38.3	5.00	0.25
	1/25/88	1646	44.8		0.25
	10/24/88	1630	53.3		1.5
1N	12/6/87	0940	44.0	6.40	0.25
	1/25/88	1633	52.0		0.25
	10/24/88	1650	61.3		0.25
1O	11/25/87	1515	31.9	7.40	0.5
	12/5/87	1621	40.2		0.5
	1/25/88	1622	46.4		0.25
	10/24/88	1633	49.4		1.0
1P	11/25/87	1400	42.0	8.40	1.0
	12/5/87	1609	52.8		0.25
	1/25/88	1615	62.3		0.25
	10/24/88	1615	71.2		
1Q	11/25/87	1323	41.0	9.80	1.0
	11/27/87	1520	45.7		0.25
	12/5/87	1553	52.5		0.25
	1/25/88	1600	62.3		0.25
	10/24/88	1600	68.5		0.5

TABLE 1—*Continued*

Site	Date	Time (PST)	Disp. (CM)	KM	Uncert. (CM)
1R	11/24/87	1120	35.0	11.80	2.0
	11/24/87	1748	38.5		0.25
	11/25/87	1435	45.0		0.25
	11/27/87	1545	48.5		0.25
	12/5/87	1018	56.3		0.25
	1/25/88	1230	69.0		1.8
	2/8/88	1145	68.6		2.0
	10/24/88	1425	77.5		0.5
1S	12/5/87	1040	45.1	12.10	3.0
1T	12/5/87	1100	63.0	12.40	1.0
1U	11/25/87	1402	48.5	12.60	3.0
	12/5/87	1136	59.5		3.0
	1/25/88	1311	70.7		
	2/8/88	1215	70.1		1.0
	10/24/88	1445	75.3		0.5
1V	12/6/88	1145	53.2	12.70	0.75
	1/25/88	1355	62.7		0.25
1W	12/6/87	1317	53.0	13.00	2.0
1X	12/6/87	1321	43.0	13.40	1.0
	1/25/88	1445	53.4		0.25
	10/24/88	1500	58.2		2.0
1Y	11/27/87	1620	13.0	13.90	0.25
	12/5/87	1335	14.0		0.25
	1/25/88	1500	15.9		1.0
	10/24/88	1320	17.1		0.5
1Z	12/5/87	1450	9.5	14.90	0.50
	1/25/88	1420	9.2		0.50
	10/24/88	1530	10.8		0.4
1AA	1/26/88	1130	0.4	15.60	0.20
2A	12/5/87	1230	0.4	12.20	0.10
2B	12/5/87	1215	3.0	12.40	0.20
	1/25/88	1258	3.4		0.20
2C	12/5/87	1158	1.4	12.70	0.20
	1/25/88	1350	1.5		0.20
2D	12/5/87	1250	3.5	12.90	0.20
	1/25/88	1406	3.7		0.20
2E	12/5/87	1300	3.4	13.10	0.20
	1/25/88	1425	3.4		0.20
2F	12/5/87	1315	1.8	13.25	0.20
2G	12/5/87	1330	4.0	13.35	0.20
	1/25/88	1427	4.0		0.20
2H	11/25/87	1325	30.0	13.85	0.20
	11/27/87	1620	33.0		0.35
	12/5/87	1347	39.8		0.75
	1/25/88	1505	49.0		0.25
	10/24/88	1430	55.7		1.0
2I	11/25/87	1310	33.0	14.30	1.0
	12/5/87	1420	43.3		1.0
	1/25/88	1508	52.0		1.0
	10/24/88	1400	64.5		1.5
2J	11/25/87	1255	30.9	14.50	1.0
	12/5/87	1425	38.9		1.0
	1/25/88	1450	49.9		1.0
	10/24/88	1330	61.4		1.0
2K	11/25/87	1245	30.0	14.80	0.25
	12/5/87	1435	38.2		0.25

TABLE 1—*Continued*

Site	Date	Time (PST)	Disp. (CM)	KM	Uncert. (CM)
	1/25/88	1408	51.4		0.25
	10/24/88	1300	59.7		1.0
2L	11/25/87	1200	31.0	15.30	1.0
	12/5/87	1452	43.6		0.25
	1/25/88	1330	51.7		0.25
	10/24/88	1230	62.5		0.5
2M	11/24/87	1730	24.0	15.50	2.0
	11/25/87	1120	28.5		0.25
	11/27/87	1637	33.4		0.25
	12/5/87	0932	39.7		0.25
	1/25/88	1320	51.6		0.25
	1/28/88	1121	52.5		0.25
	4/13/88	1838	57.2		0.25
	8/3/88	1820	61.1		0.5
	10/24/88	1200	61.9		0.5
2N	11/25/87	1345	32.5	15.70	1.0
	12/5/87	0922	44.0		1.0
	1/25/88	1308	55.1		0.20
	10/24/88	1140	64.0		0.5
2O	11/25/87	1125	37.5	16.0	0.50
	12/5/87	0858	50.3		0.20
	1/25/88	1255	61.2		0.20
	10/24/88	1120	71.6		0.5
2P	11/25/87	1100	38.7	16.70	1.0
	12/5/87	0842	50.7		0.20
	1/25/88	1245	61.4		0.20
	10/24/88	1100	72.2		1.0
2Q	11/25/87	1035	45.8	17.40	0.30
	12/5/87	0820	58.8		0.20
	1/25/88	1235	71.0		0.20
	10/24/88	1040	85.5		0.8
2R	11/25/87	1025	40.5	17.60	1.5
	12/5/87	0810	53.7		0.20
	1/25/88	1210	61.2		0.20
	10/24/88	1020	75.9		0.5
2S	11/25/87	0945	38.3	18.35	0.25
	12/5/87	0743	52.5		0.20
	1/25/88	1140	65.0		0.20
	10/24/88	1000	76.0		0.5
2T	11/24/87	0800	28.0	18.60	2.0
	11/24/87	1656	34.0		2.0
	11/25/87	0913	39.0		2.0
	11/27/87	1655	45.0		2.0
	12/6/87	1420	53.5		0.30
	12/9/87	1020	55.3		0.40
	12/16/87	1420	58.0		0.25
	1/25/88	1110	64.3		0.25
	1/28/88	1110	65.5		0.30
	2/8/88	1100	67.1		0.60
	4/13/88	1815	69.9		0.25
	8/3/88	1810	73.7		0.5
	10/24/88	0900	74.0		0.5
2U	11/24/87	0725	18.3	19.10	0.75
	11/24/87	1359	25.3		0.25
	11/24/87	1640	27.3		0.25
	11/25/87	0855	30.8		0.25

TABLE 1—*Continued*

Site	Date	Time (PST)	Disp. (CM)	KM	Uncert. (CM)
	11/25/87	1653	31.0		0.25
	11/27/87	1200	36.2		0.25
	12/6/87	1435	44.3		0.25
	12/9/87*	0830	45.5		2.0
	12/16/87	1615	49.5		2.0
	1/26/88	1200	57.6		2.0
	2/8/88	1345	60.8		2.0
	8/3/88	1836	68.2		2.0
	10/24/88	0830	70.3		2.0
2V	11/24/87	1414	35.5	19.25	4.0
	11/25/87	0916	40.5		0.25
	11/27/87	1210	46.0		0.25
2W	11/24/87	1435	25.2	19.35	4.0
	11/24/87	1626	26.0		4.0
	11/25/87	0928	30.2		1.0
	11/27/87	1220	35.7		1.0
	12/6/87	1720	43.2		1.0
	1/25/88	1640	48.2		1.0
2Y	1/24/87	1511	34.0	20.10	2.0
	11/25/87	0956	39.2		0.25
	1/25/88	1000	60.6		0.25
	10/24/88	1030	71.7		2.0
2Z	11/24/87	1537	31.0	20.60	3.0
	11/25/87	1021	35.0		3.0
	12/6/87	1657	48.3		0.25
	1/25/88	1017	58.0		0.25
	10/24/88	1100	65.2		1.0
2AA	1/24/87	1853	14.0	20.65	2.0
	1/25/87	1029	17.0		2.0
	12/6/87	1646	29.0		2.0
2BB	11/24/87	1520	18.0	22.20	1.0
	11/25/87	0809	20.6		0.25
	12/6/87	1623	29.3		0.25
	1/25/88	1115	36.5		0.25
	10/24/88	1135	42.7		0.5
2CC	11/25/87	0800	12.5	22.80	0.50
	11/27/87	1128	15.3		0.20
	12/6/87	1615	19.0		0.20
	1/25/88	1100	20.8		0.20
	10/24/88	1200	25.7		0.5
2DD	11/25/87	0736	7.75	23.10	0.25
2EE	11/24/87	1600	7.6	23.25	0.20
	11/25/87	0744	8.8		0.20
	11/27/87	1119	10.3		0.20
	12/6/87	1605	13.5		0.20
	1/25/88	1020	17.2		0.20
	10/24/88	1230	23.7		0.5
2FF	11/24/87	1400	6.5	23.35	0.50
	11/25/87	0719	8.5		0.50
	11/27/87	1110	10.0		0.50
	12/6/87	1558	11.2		0.50
	1/25/88	1035	14.3		0.75
	10/24/88	1300	16.7		1.0
2GG	11/24/87	1430	3.0	23.65	0.40
	11/25/87	0706	3.0		0.40
	12/6/87	1537	4.0		0.20

TABLE 1—*Continued*

Site	Date	Time (PST)	Disp. (CM)	KM	Uncert. (CM)
	1/25/88	0905	6.5		0.50
	10/24/88	1318	6.7		0.25
2HH	11/24/87	1415	1.0	23.75	0.20
	11/25/87	0655	1.0		0.20
	11/27/87	1059	1.0		0.20
	12/6/87	1530	1.0		0.20
	1/25/88	1010	1.0		0.20
2II	1/25/88	0915	2.5	23.70	0.20
2JJ	1/25/88	0930	1.3	23.90	0.20
2KK	1/25/88	0945	1.4	24.00	0.20
2LL	1/25/88	1000	0.1	24.05	0.10

* Monument 2U moved 20 m southeast on 6 December 1987.